
HIGH FREQUENCY RADAR OBSERVING SYSTEM SIMULATION EXPERIMENT IN THE WESTERN MEDITERRANEAN SEA: A LAGRANGIAN ASSESSMENT APPROACH.

Jaime Hernández-Lasheras

CMCC Foundation - Euro-Mediterranean Center on Climate Change, Italy.
jhlasheras@gmail.com

Alex Santana

Balearic Islands Coastal Observing and Forecasting System (SOCIB), Palma, Spain

Baptiste Mourre

IMEDEA (CSIC-UIB) - Instituto Mediterraneo de Estudios Avanzados. Esporles, Spain
Balearic Islands Coastal Observing and Forecasting System (SOCIB), Palma, Spain

Ismael Hernandez-Carrasco

IMEDEA (CSIC-UIB) - Instituto Mediterraneo de Estudios Avanzados. Esporles, Spain

Alejandro Orfila

IMEDEA (CSIC-UIB) - Instituto Mediterraneo de Estudios Avanzados. Esporles, Spain

June 7, 2024

ABSTRACT

The impact of the expansion of a high-frequency radar (HFR) system in the Ibiza Channel (Western Mediterranean Sea) is evaluated through an Observing System Simulation Experiment (OSSE). The installation of two new antennas in the Iberian Peninsula would complement the existing ones in the islands of Ibiza and Formentera, providing surface currents observations of the full channel. Two different configuration of the same model, validated to give realistic simulations, are used: i) a Nature Run (NR) which is considered as the real ocean state and that is used to generate pseudo-observations, and ii) a Control Run (CR) in which we will assimilate the pseudo-observations. The OSSE is first validated by comparison against a previous Observing System Experiment (OSE). The effect of the new antennas for forecasting surface currents is evaluated in two different periods. The effect of the new antennas is relatively small when the NR and CR depict a similar circulation. However, in situations where both models present higher differences, the error reduction with respect to the use of only the actual system can be of up to 19%. The effects on the transport in the area are also analyzed from a Lagrangian perspective, showing that DA can help to better represent the Lagrangian Coherent Structures present in the NR and constrain the ocean dynamics.

Keywords Data Assimilation · High-frequency radar · Operational oceanography · Regional modelling · Lagrangian validation

1 Introduction

Observations, models and data assimilation (DA) are the three key elements in operational oceanography. Combining them in an optimal way and bridging synergies between the different research communities is key to advance our knowledge of the oceans and be able to answer to societal needs for a sustainable development [33, 45].

In this sense, Ocean Observing Systems (OOS) play a key role, and numerous efforts have been made all over the world to enhance its development and strengthen the collaboration within the scientific community [38, 28, 6]. In particular, in Europe, several initiatives have been made or are ongoing to provide better answers to science and to societal challenges (e.g., CMEMS programme, Jerico and Eurosea projects) [9, 25, 41].

The rising capabilities of remote sensing and the development during the last decades of *in-situ* observing programs such as Argo [24], allowed a better understanding of ocean processes at multiple scales. In coastal areas, Regional Ocean Observing Systems (ROOS) are nowadays providing near real time observations combining observations from moored instruments, periodic cruises, autonomous vehicles, Lagrangian platforms or high-frequency radars (HFR), among others.

Numerical models provide a complete view of the three dimensional structure of the ocean. However, they are inevitably affected by errors from parametrization of non resolved physical processes, discretization issues, or the lack of accurate forcing. To improve reliability, numerical models for operational purposes should be fed with observations through data assimilation. Observing System Experiments (OSEs) assimilating data are numerical experiments that can be designed to evaluate the capability of specific observing systems and eventually correct model forecasts on simulations. Similarly, the potential impact of observing system has to be evaluated to help design these systems. Observing System Simulation Experiments (OSSEs) can be performed to help to optimally design an OOS or a future campaign [22].

OSSEs were first developed for the atmospheric science community, and over time, specific design criteria have been developed to ensure the realism of the assessments performed, as defined in [2]. In ocean studies multiple OSSEs had been done, however, most of them did not use a full-fledged DA system approach for the evaluation. Generally, Kalman filters, empirical orthogonal functions (EOF) based or different interpolation methods were used to map the observations and reconstruct the ocean state [11, 3, 34]. Following the procedure established for atmospheric studies [19], [12] applied them for the first time in the ocean, and in the last years, several studies have been done following the criteria exposed in that work, as we will do here. For instance, [10] performed an evaluation of the influence of the future deep Argo float network, and [4] assessed the impact of the assimilation of data from the future SWOT satellite mission in a global-high-resolution model.

In the fraternal twin OSSE approach employed, two models are required: (i) one, hereinafter referred to as Nature Run (NR), which is considered to represent the true ocean and that will be used for validation and to extract the pseudo-observations, and (ii) the model we would like to correct with the assimilation of such pseudo-observations. To be credible, the OSSE should satisfy the following design criteria and rigorous evaluation steps: (a) The models should be validated to give realistic simulations and the pseudo-observations generated in a way that resemble the real ones, including the observation errors, that need to be specifically added. (b) The validation should be performed by comparison to a previous OSE where real observations are assimilated. The same observations should be assimilated in both experiments, except for the fact that, in the OSSE, the pseudo-observations are synthetically generated from the NR. (c) If the impact assessment is consistently the same, we consider the OSSE to be validated.

In the OSSE framework the ocean state is fully known. This permits to assess the impact in regions that normally are not sampled or to experiment additional validation techniques. For instance, we can use Lagrangian techniques for the assessment of transport and the ocean dynamics, such as the Lagrangian Coherent Structures (LCS) obtained from the Finite Size Lyapunov Exponents (FSLE) [8, 13]. Ridges of FSLE field reveal LCS, which act as transport barriers. These LCS have been proven to be useful to understand ecological processes, such as nutrients distribution, or oil-spill and search and rescue operations [15, 27, 35].

Normally, the validation of these Lagrangian techniques is limited. LCS computed from model simulations can be compared to those calculated from geostrophic currents derived from altimetry products [17] which suffer limitations when approaching the coast [44, 30]. Also from HFR measured currents [15], that are limited to cover small coastal areas. The validation of LCS can be performed by comparison with active tracers, as chlorophyll filaments [26, 15], which by their nature can not depict the full structures present in the ocean; SST fronts [8], which are inferred from satellite products that can be affected by clouds; or fish stock concentrations [7], tracked seabirds or marine predators [21], that are difficult to monitor. Here we will take profit of the full ocean state knowledge supposed in the OSSE approach. The use of a NR model for the validation of the LCS computed from the model simulations implies a step forward to address the question of how data assimilation can help models to correct the circulation, especially in coastal areas.

This study is a continuation of the work presented in [16], where a series of OSEs were performed to evaluate the impact of HFR DA on the correction of surface currents in the Ibiza Channel (IC). In that work, it was shown that using HFR observations together with satellite observations (altimetry and sea surface temperature) and Argo temperature and salinity profiles increased the model’s capability to forecast surface currents. In this work we will use the same set-up, using the nudging initialization method described in the mentioned work, as it is the configuration employed in the WMOP, the Western Mediterranean OPERational forecasting system.

The paper is structured as follows; Section 2, presents the data, the general set-up of the OSSE and the Lagrangian approach that will be followed. In Section 3, the OSSE performance is presented as well as the performance in the Eulerian and Lagrangian frameworks. The next sections discuss the main results and conclusions of the work.

2 Data and Methods

2.1 Study Area and HFR system

Our region of study is the Ibiza Channel (IC), in the Western Mediterranean Sea. The modelling area spans from Gibraltar strait in the west to Sardinia and Corsica in the east. The IC is a passage of water between the Iberian peninsula and the island of Ibiza, in the western Mediterranean Sea [31, 32]. It is a choke point between the saltier waters from the north, that generally flow along the coast, and the incoming fresher waters from the south [18].

SOCIB operates since 2012 two CODAR HFR antennas in the islands of Ibiza and Formentera, measuring surface currents in an area up to 80 km far off the coast [40]. Here we evaluate the potential impact that a couple of new antennas eventually installed in the Iberian peninsula, in the eastern part of Cape la Nao (Fig. 1), would have in the WMOP system. By installing these new antennas, the IC HFR system will expand its coverage area covering the entire channel. The area, shown in Fig. 1 (red dashed line), is considered as the most likely coverage in terms of total velocities ($u-v$) that a couple of antennas in the peninsula will provide together with the actual system.

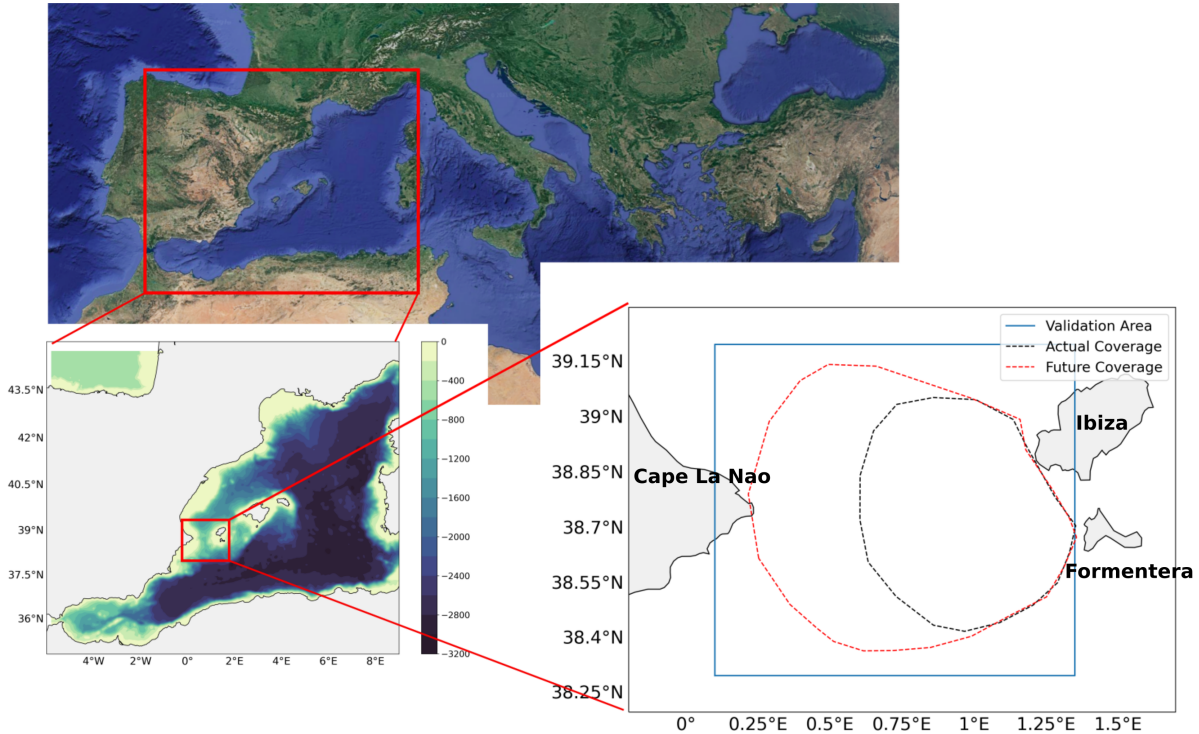


Figure 1: WMOP domain and bathymetry in the Western Mediterranean. HFR actual coverage area (black dashed) and Future one (red dashed) from which observations have been simulated. The area selected for validation is also shown (blue).

2.2 OSSE set-up: Simulations

The OSSE perspective requires two model simulations. Here we used a fraternal twin OSSE system approach [12], in which two different configurations of the same model are employed: i) a Nature Run (NR), which is considered to represent the true ocean and that will be used for validation and to extract the pseudo-observations, and (ii) a Control Run (CR) model in which we will evaluate the impact of assimilating different observing sources. We use the WMOP [20] model, which is a regional configuration of ROMS [36] for the Western Mediterranean Sea. It spans from Gibraltar Strait in the west to Corsica and Sardinia straits in the east, with a horizontal resolution around 2 km and 32 vertical terrain-following sigma levels (resulting in a vertical resolution between 1 and 2m at the surface). Both the NR and the CR model, which will be used to assimilate, have the same configuration, parametrization and atmospheric forcing, with the only difference in the initial state and the boundary conditions used in each of them. The CR is a free-run hindcast simulation developed and evaluated in [29, 1]. We will use this model configuration to assimilate data into, as it is the same one used in the reference OSE we will use for validation [16]. It uses the Copernicus Marine Forecasting System for the Mediterranean Sea (CMEMS MED-MFC), with a $1/16^\circ$ horizontal resolution [37], as initial and lateral boundary conditions. NR, in contrast, uses the Mercator Glorys reanalysis global product, with a $1/12^\circ$ horizontal resolution (CMEMS GLOBAL_REANALYSIS_PHY_001_030) and has also been validated to give realistic simulations, comparing against observational data from satellites and Argo buoys. The atmospheric forcing, common for both simulations, is provided every 3 hours at $1/20^\circ$ resolution by the Spanish Meteorological Agency (AEMET) through the HIRLAM model [42] and the bathymetry is derived from a $1'$ database [39].

Both model realizations resolve the same scales, while differing in the mesoscale structures present during the experiment period, which are the two main initial requirements needed for a fraternal twin OSSE approximation. Figure 2 shows the Hovmoller diagram of the meridional velocity in a transect across the Ibiza Channel (latitude 38.77°N), where we can observe differences between both runs in the currents across the IC during the whole year 2014. The mean circulation pattern in the Ibiza Channel between 21 September and 20 October are shown in the top two panels of Fig. 3, where we have also marked (dotted line) the coverage areas of the actual and the possible future antennas considered in this study. Both simulations present in average a southward current at the western side of the IC, while having a northward flow in the eastern part. In the case of the NR both flows are more intense than in the CR, which depicts a more intense eastward current in the southern part of the coverage area.

To further explore the capabilities of the new antenna under different possible circumstances, we selected another period in which the dynamics in the area from the two simulations presented more differences. For this, we chose August 2014 to repeat our simulations. In the CR simulation, the dynamics during August are similar to the following September-October period, with northward currents in the east side of the channel and southward in the west, as can be seen in Fig. 2. On the contrary, the NR depicts a northward current in the eastern side of the channel and also in the west, where it is more intense. In the middle of the channel (0.62°E - 0.85°E), there is a strip of weak northward current neither present in the CR. Top two panels of Fig. 4 shows the mean circulation in the region for the NR and CR.

For the two commented periods we run three data assimilative simulations, using different datasets, and we evaluate the impact comparing against the free-run CR (Table 1). We called GNR the simulation assimilating the generic data set, composed of SLA along-track, SST and Argo T-S profiles. H-A and H-F are the simulations that, additionally to this generic data-set, employ HFR simulated total observations from the actual or the future coverage area, respectively.

The data assimilation system employed is the Local Multimodel EnOI scheme previously described that was validated to correctly assimilate HFR observations in [16]. We here use the nudging initialization method after analysis, as it is the one employed in the WMOP operational system and it is less prone to produce discontinuities in the field which could affect the computation of FSLE, that will be later presented.

Simulation	Assimilated observations
NR	None. Pseudo-reality
CR	None
GNR	SLA, SST, TS
H-A	SLA, SST, TS, HFR (actual coverage)
H-F	SLA, SST, TS, HFR (future coverage)

Table 1: Basic description of the experiments, indicating the dataset used in the simulations.

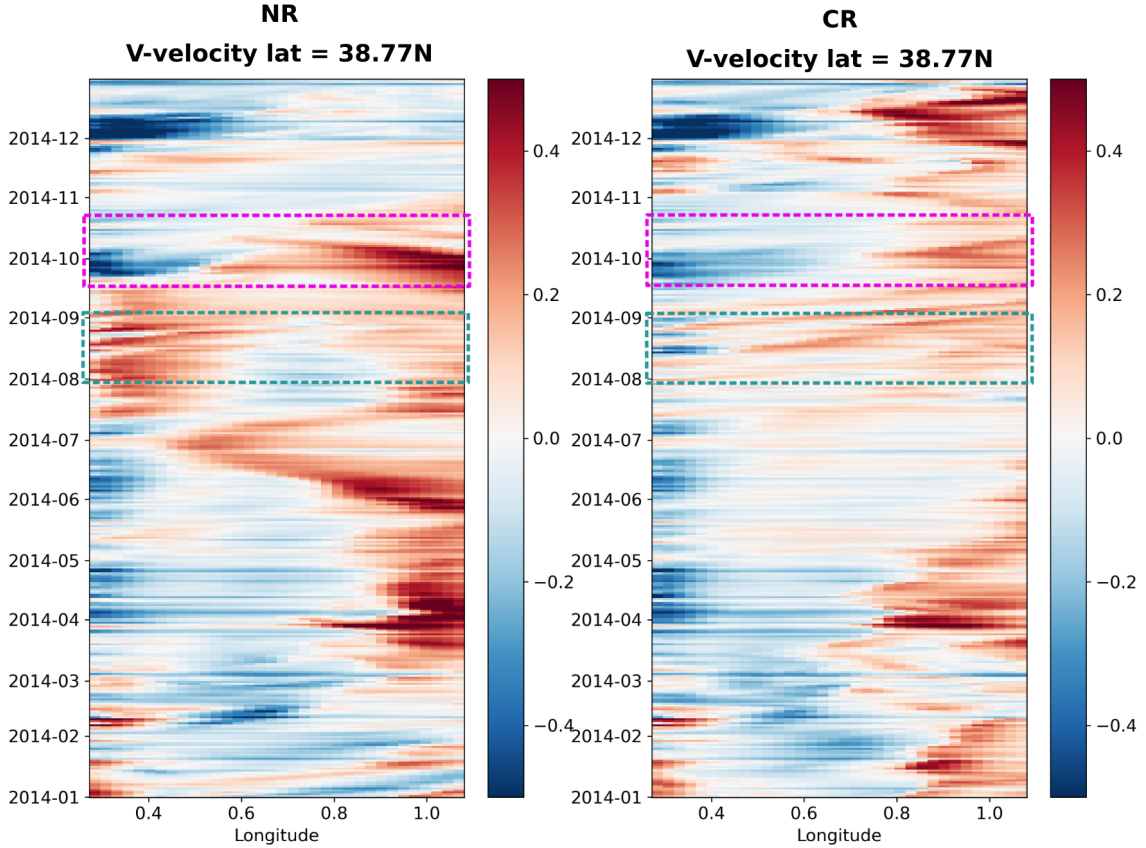


Figure 2: Hovmoller of the meridional component of velocity during 2014 for a transect at 38.77N latitude, in the Ibiza Channel, for NR (left) and CR (right). The two periods of the OSSE are highlighted. The period coincident with the OSE is marked in pink (21 September to 20 October). In green, the second period simulated, during August 2014.

	Representation	Instrumental
SLA (m/s)	0.03	0.02
SST (°)	0.25	0.5
Argo - T (°)	0.25	0.1
Argo - S	0.05	0.01
HFR (m/s)	0.03	0.02

Table 2: Representation and instrumental errors employed for the different observations.

2.3 OSSE Set-up: Pseudo-Observations

For our experiment, the satellite and Argo pseudo observations have been extracted at the same position and time as the real observations in the previous chapter’s OSE [16], that is considered as reference. We simulated along-track sea level anomalies (SLA) from four different altimeters (Cryosat, Jason-2, Saral Altika, and HY-2). NR fields are interpolated in space and time to each satellite observation after removing the mean dynamic topography. For SST, we emulate the SST Foundation product, which does not account for the diurnal cycles, sub-sampling surface temperature fields from the NR at 8 a.m., with a 10 km resolution. The Argo profiles were sampled by interpolating the temperature and salinity fields in space and time. We added noise to every observation, which was randomly generated for each observation considering a Gaussian probability distribution with a standard deviation of the value of the error. The observation error has been considered the same as for the real observations. Table 2 indicates the value of the representation and instrumental errors considered for the different observations. For Argo observations only the horizontal representation error is shown. Note that the total error has the expression $\sigma_{tot}^2 = \sigma_{rep}^2 + \sigma_{ins}^2$.

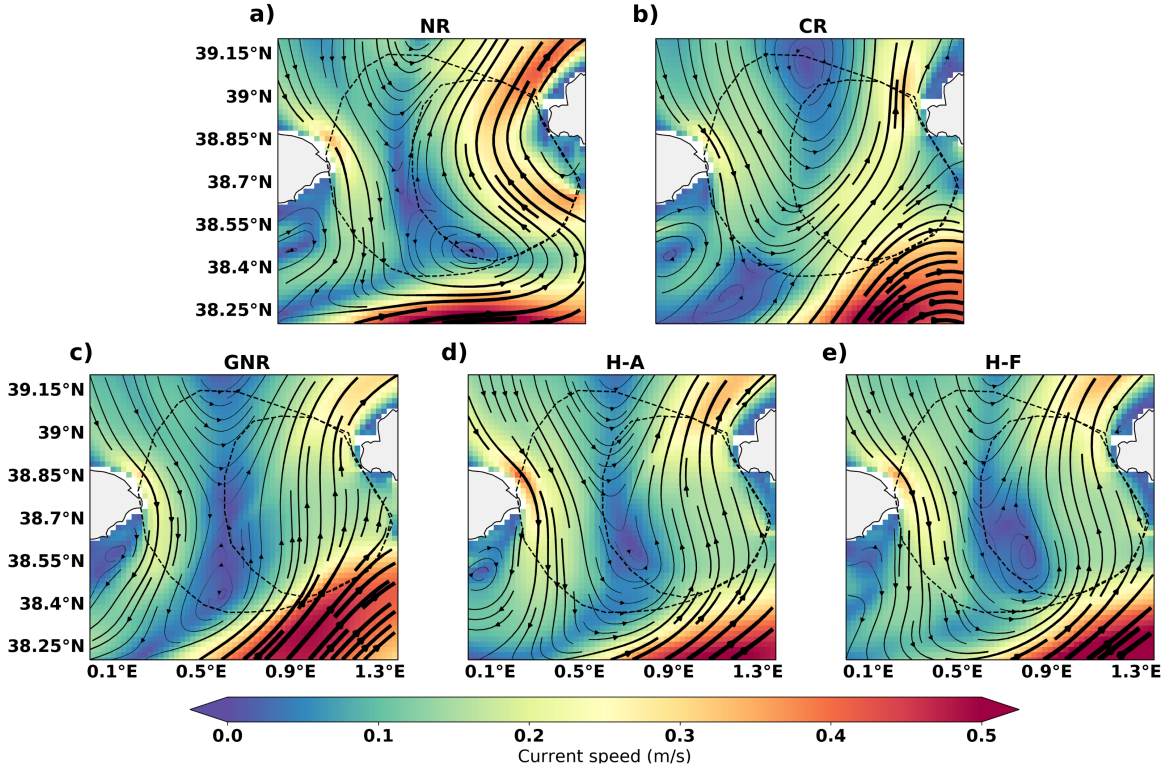


Figure 3: Mean surface circulation during the one-month simulation (20-September to 20-October) in the Ibiza Channel for the a) Nature Run (NR), b) Control Run (CR), c) GNR, d) H-A, e) H-F. Actual and future coverage areas are marked in dashed black lines.

	SLA (cm)		SST (°C)		Argo T (°C)		Argo S	
	mean	std	mean	std	mean	std	mean	std
OSE	0.07	0.05	0.01	0.62	-0.15	0.90	-0.00	0.21
OSSE	0.01	0.06	-0.01	0.78	-0.02	0.81	-0.03	0.19

Table 3: Mean value and standard deviation of the Innovations of SLA, SST and Argo T-S for the OSE and OSSE.

The histogram of the innovations (observation - model) is shown in Fig. 5 for the OSE (blue) and OSSE (red), whose results are also synthesized in Table 3. We can observe that all observations follow a similar distribution both for OSE and OSSE. The only discrepancy is found in the SLA, where we can observe a bias of 0.07 m in the OSE. This is a known issue concerning the value of the satellite SLA observations. Satellite SLA observations are computed by extracting the value of the absolute dynamic topography measured by the satellite to the mean dynamic topography (MDT). The MDT of the model generally differs from the MDT of the observations. Moreover, two different simulations have two different MDTs. The rise of the mean sea level generates a climatological trend in the observations which has not been corrected and thus, SLA observations from recent years present a positive bias which also affects the innovations. However, we believe this does not significantly affect the assimilation of SLA, as it is not corrected during the simulation (as discussed in the previous chapter [16]) and do not impact the geostrophic circulation. The values of the innovations standard deviation, which is directly related to the centered-root-mean-square-deviation (CRMSD), has small differences between OSE and OSSE for all observing sources.

For the HFR observations we have followed a slightly different approach. We have considered two polygons, one containing the actual coverage area and another considering the potential future coverage that a set of two antennas settled in the western part of the IC might provide, according to expert criteria (Fig. 1). Within these areas, we have sub-sampled the daily mean velocity fields of the NR in a spatial grid of 3 km resolution, which corresponds to the HFR total (u-v) observing resolution in the area [40]. We randomly dismissed 15% of the observations for simulating potential gaps in the antennas coverage. Again, we have introduced a Gaussian noise to the observations and considered

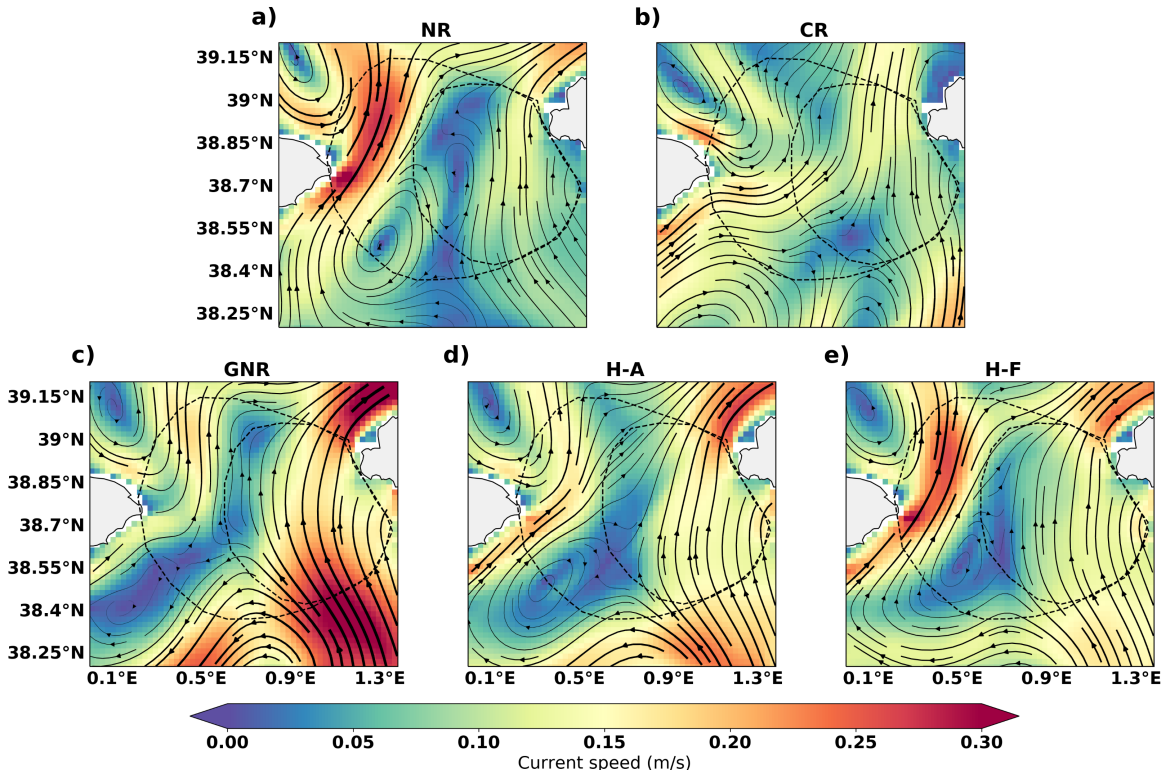


Figure 4: Mean surface circulation during the one-month simulations (August 2014) in the Ibiza Channel for the a) Nature Run (NR), b) Control Run (CR), c) GNR, d) H-A, e) H-F. Actual and future coverage areas are marked in dashed black lines.

the same instrumental and representativity error we previously used with the real data. Fig. 6 shows the histogram of the innovations for both variables of velocity during the two periods run.

It can be observed that during the period of 21 September to 20 October, coincident with the previous OSE, the innovations present a larger discrepancy, both in mean and standard deviation, as seen in the spread of the distribution. During this period, the model tends to overestimate the meridional currents observed by the HFR. However these discrepancies are not systematic, as can be seen for the period of August, where the innovation distribution is much more similar when using real or virtual observations. While the meridional component still has a mean difference, the standard deviation is almost equal whether using real or virtual observations for both velocity components.

Overall, the statistical properties of the innovations are consistent between the OSE and the OSSE, which validates the use of the NR to generate pseudo-observations. The validation of the OSSE framework employed will be further completed, assessing the impact of the observations on the model.

2.4 Lagrangian Analysis.

The effects in the transport are here assessed using a Lagrangian approach. In the Lagrangian framework one has the advantage of exploiting both spatial and temporal variability of a given velocity field [13]. In particular, we will use the finite size Lyapunov exponents (FSLE) where a set of fluid particles, initially separated a distance δ_0 , are transported by the flow and followed in time by integrating the equation of motion. The FSLE, denoted by λ (Eq. 1), is inversely proportional to the time at which two fluid particles initially separated δ_0 get separated a certain distance δ_f . When integrated backwards, high values of FSLE are identified as limits of maximum stretching. The so-called Lagrangian Coherent Structures (LCS) are the ridges of FSLE fields, which act as transport barriers.

The integration of the trajectories is performed with OceanParcels [23], using a Runge-Kutta 4 algorithm with an integration time step of 1 hour. The initial separation distance δ_0 is considered equal to the model grid resolution (around 2 km). The final distance $\delta_f = 10 \cdot \delta_0$, as considered optimal in other studies which explore the importance of

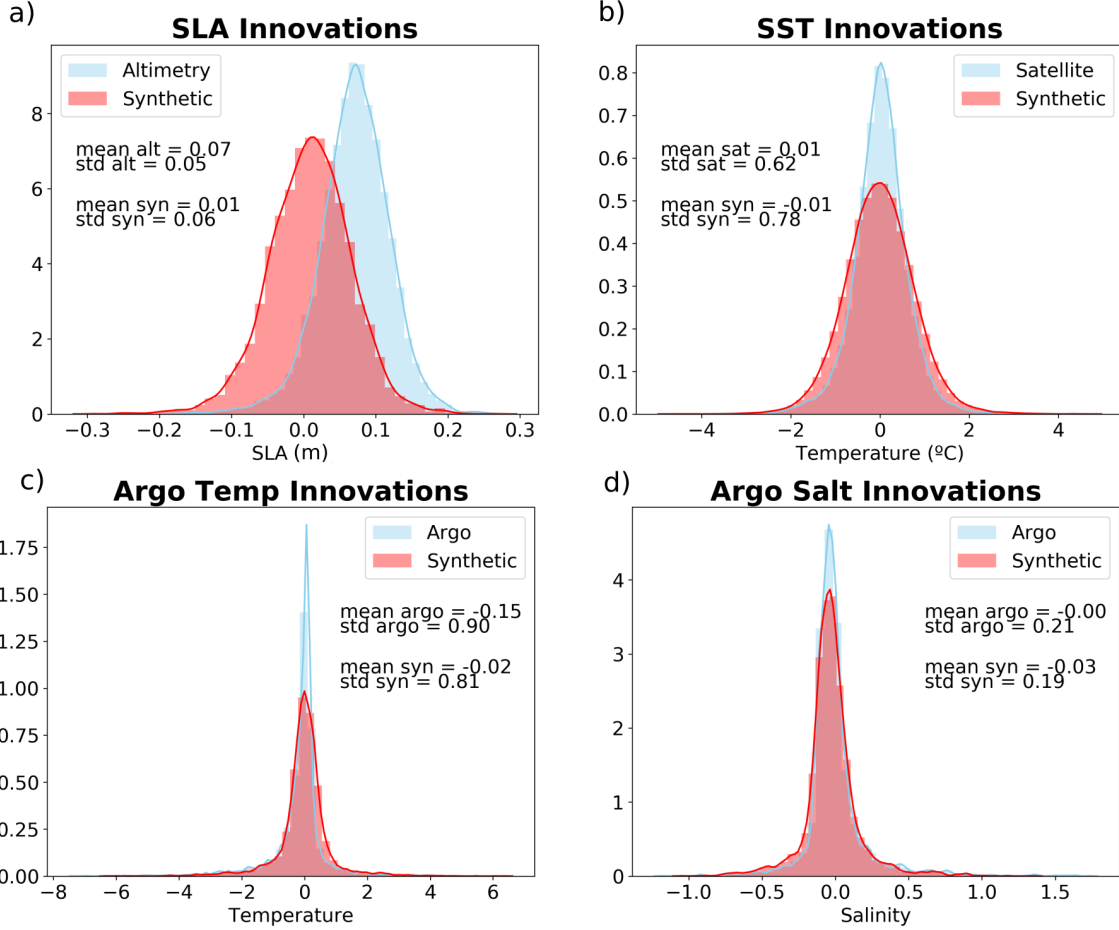


Figure 5: Histograms comparing the innovations (observation - model) for OSE (blue) and OSSE (red) for the different observing sources: a) SLA along track, b) SST, c) Argo temperature profiles, d) Argo salinity profiles.

this parameter [13, 14],

$$\lambda(\mathbf{r}, t, \delta_0, \delta_f) \equiv \frac{1}{\tau} \log \frac{\delta_f}{\delta_0}. \quad (1)$$

We calculated the FSLE field in the entire domain, launching particles with an initial separation equal to the model grid size. For the one-month simulations, we computed the FSLE integrating the trajectories backwards in time during 15 days. From the 16th simulation day onward, the last 15 days' fields are used to obtain one FSLE field.

3 Results

3.1 OSSE validation: Comparison with OSE.

First, we assess the results of our experiments comparing them to the ones obtained in the previous chapter's OSEs used as reference [16]. When the forecast error reduction obtained with both perspectives (OSE and OSSE) is similar, we can consider the system is valid, and reliably estimates the impact of other potential observations. This would enhance our reliability in the assessment of the future observation system design. For this validation we analyze the period spanning from 21 September to 20 October from an Eulerian perspective, in a similar way as it was done in the previous OSE: a) For SLA, we compare for each day of simulation the model equivalents against the NR at every location of all along-track possible observations in the region; b) SST comparison between model and NR is performed at every observation point within a grid of 10 km resolution, like the one used to generate the pseudo-observations; c) Temperature and salinity fields are interpolated in time and space to the Argo float profile observations; d) For comparison against HFR data we interpolate the surface average fields to the position of the real observations. Note

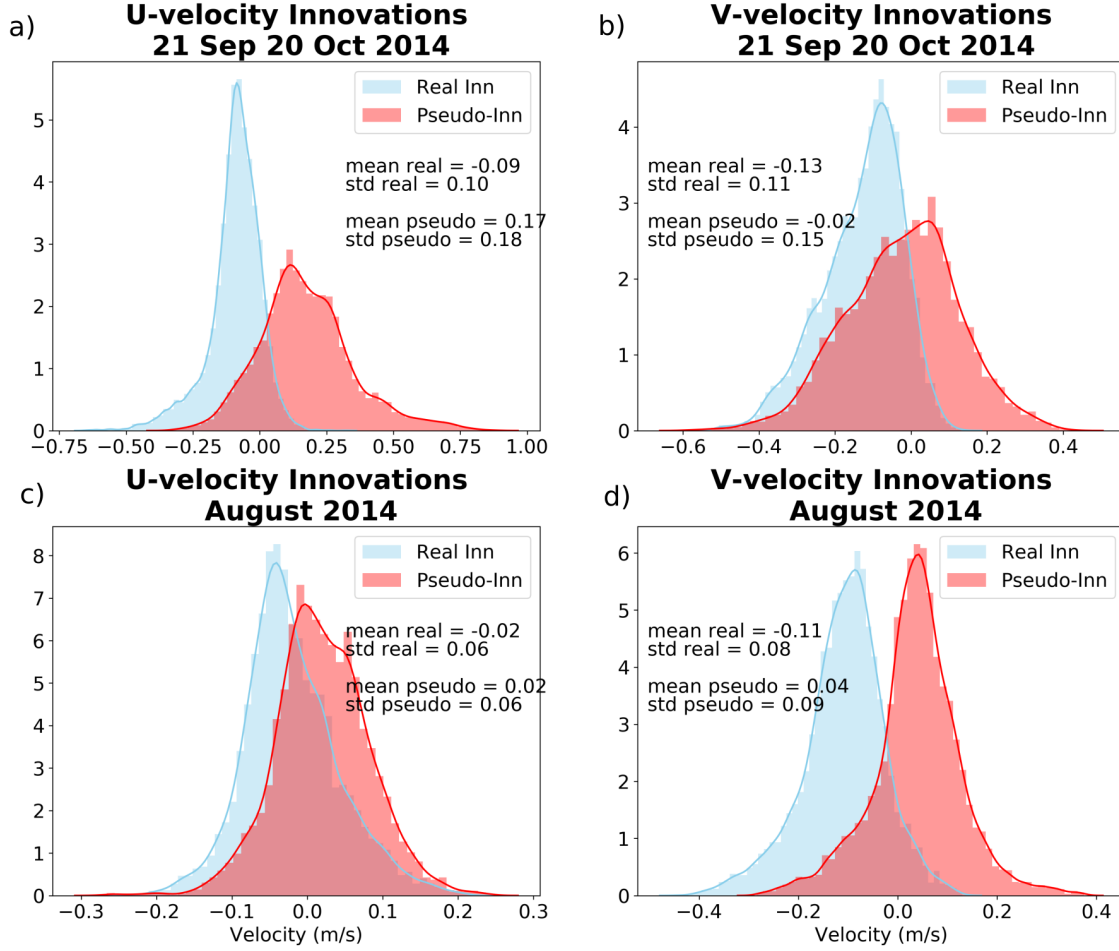


Figure 6: Histograms comparing HFR Pseudo-obs created from NR against real observations assimilated in previous OSE: a) zonal velocity, b) meridional velocity.

that in the OSSE perspective, we compare against the value of the true ocean state, represented by the NR simulation. Thus, although the evaluation with the NR is done at some of the same points from where we extract the assimilated observations, the validation can not be considered as fully independent.

Table 4 shows for each observing source the CRMSD normalized with the CR for the OSE and OSSE. This metric give us an overview of the impact, without taking into account the mean error (bias), which is only significant in the case of SLA observations, as was commented previously (section 2.3). For SLA, SST and Argo T-S only the results of the GNR simulation are shown, as the ones obtained for H-A are almost the same when comparing against these sources. For the comparison against HFR data we show the results of GNR and H-A simulations. We can observe that the normalized CRMSD for GNR is slightly higher for the OSSE than for the OSE, with even an increase in the error for the v-component. On the contrary, H-A produces better results for the OSSE in the u-component. This suggests a bigger impact of adding HFR observations in the OSSE approach for this specific period. For the rest of observing sources we can observe that the error reduction between OSE and OSSE is of the same order.

A further analysis of the results is shown in the Taylor diagrams in Fig. 7. For SLA, the model error decreases around 40% and the correlation between model and observation increases from 0.38 to 0.75 when using DA. Results are almost equal for all three simulations using DA. For SST, the comparison between model and NR is performed at every observation point within a grid of 10 km resolution, like the one used to generate the pseudo-observations. Results show how the error reduction is around 36%, while correlation increases for all simulations from 0.87 to 0.94. These results are of the order of magnitude of the ones obtained for real observations (shown in the previous OSE). Similarly, for the Argo T-S observations, the results obtained for the OSSE are very similar and of same the order of those obtained with real-world observations. The error is reduced by 41 and a 36 %, for temperature and salinity respectively, and the correlation increases in both cases (Fig. 8).

		SST	SLA	Argo-T	Argo-S	HFR-U	HFR-V
OSE	GNR	0.69	0.73	0.66	0.62	0.80	0.96
	H-A					0.71	0.74
OSSE	GNR	0.64	0.60	0.59	0.64	0.87	1.06
	H-A					0.64	0.74

Table 4: Comparative table between OSE and OSSE experiments, of the normalized RMSD against the different observing sources. SLA, SST and Argo values are only shown for GNR simulation in each case, as the values for the H-A are the same ones.

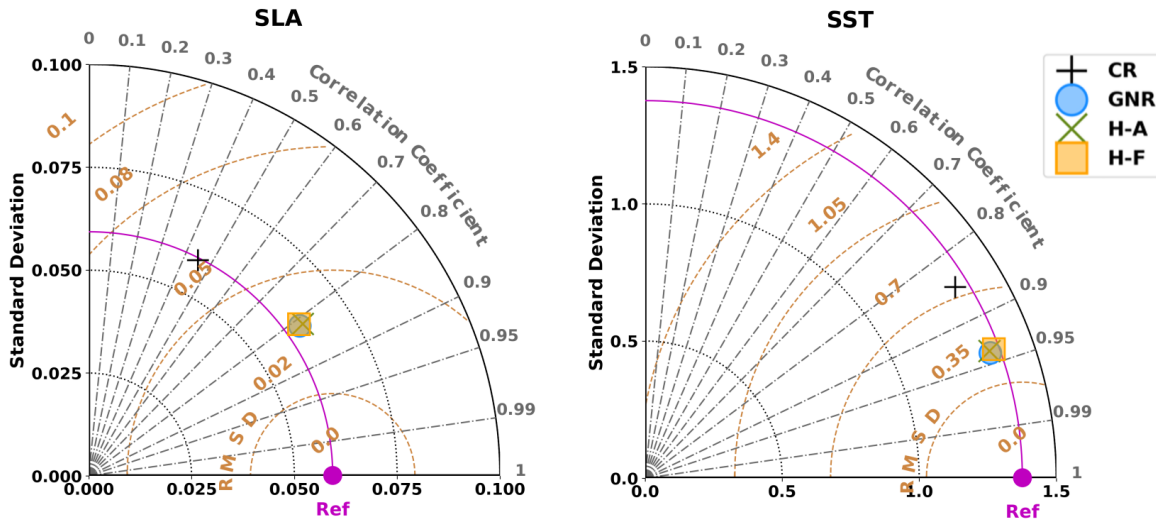


Figure 7: Taylor diagrams comparing models and NR pseudo-observations in terms of SLA (left) and SST (right) over the whole modelling domain. X and Y axis represent the standard deviations of the data. Distance from the reference point located on the X axis (noted as Ref. in magenta) represents the centered root mean square deviation (CRMSD). Correlation between observations and model increases clockwise. Symbols represent the different simulations, as specified in the legend

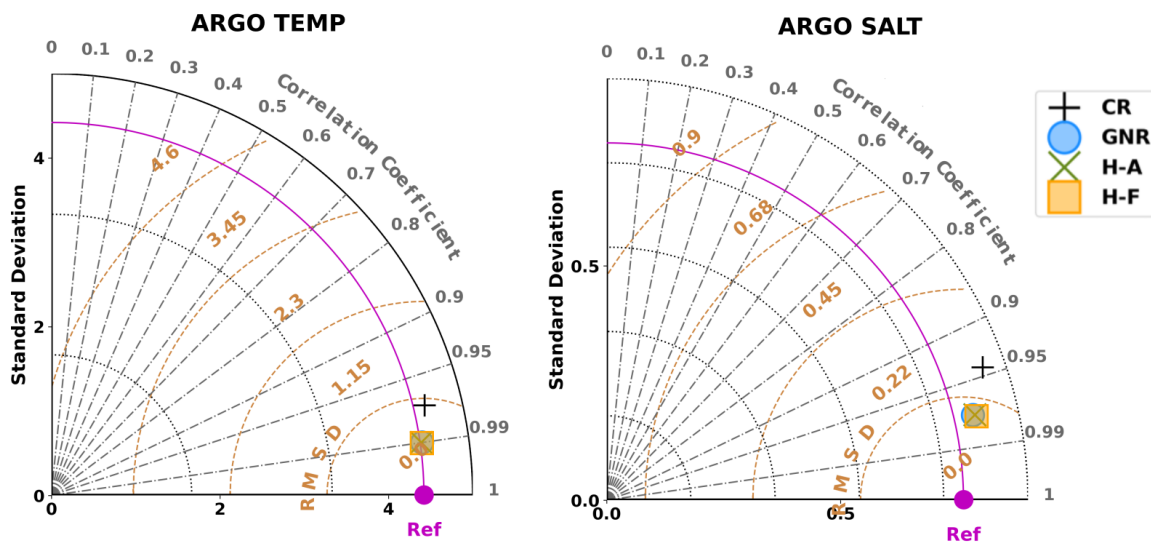


Figure 8: Same as Fig. 7 for Argo salinity and temperature

3.2 Impact of the HFR system expansion: Eulerian validation

We further assess the impact of OSSEs on the surface currents comparing the model fields in each simulation against the NR in the area of the IC. Note that the approach is different to what we previously did to validate the OSSE by comparing it to the OSE as only the data at the observing points during the coincident period were evaluated previously. The area used for the assessment in this section, which can be seen in Fig. 1, covers the entire IC, being wider than the coverage of the future HFR system. This way, we evaluate the impact of HFR DA beyond the coverage of the antennas and its effects on the transport in the region.

We evaluate the two different periods of simulation. During September-October, the meridional currents in the region are more intense, as can be seen in the Hovmoller diagram 2 and so are the errors. The assimilation of generic observations only does not improve the prediction of surface currents in the region. For the u component, GNR improves the correlation with the NR from 0.15 to 0.43 but only slightly reduces the CRMSD (centered root mean square deviation). For v, both the correlation and error are slightly degraded in comparison to CR. The use of HFR observations additionally to the generic sources is here essential to improve the forecasting of both zonal and meridional components. The improvement obtained when assimilating observations from the future HFR system is slightly better than that obtained when only using observations from the actual coverage area. Both for H-A and H-F the correlation are higher than 0.62, and the error is reduced by more than 32% for the u-component. For the v-component, the correlation for both simulations also increases with respect to the NR, and the error is reduced by 15% and 21% for H-A and H-F, respectively.

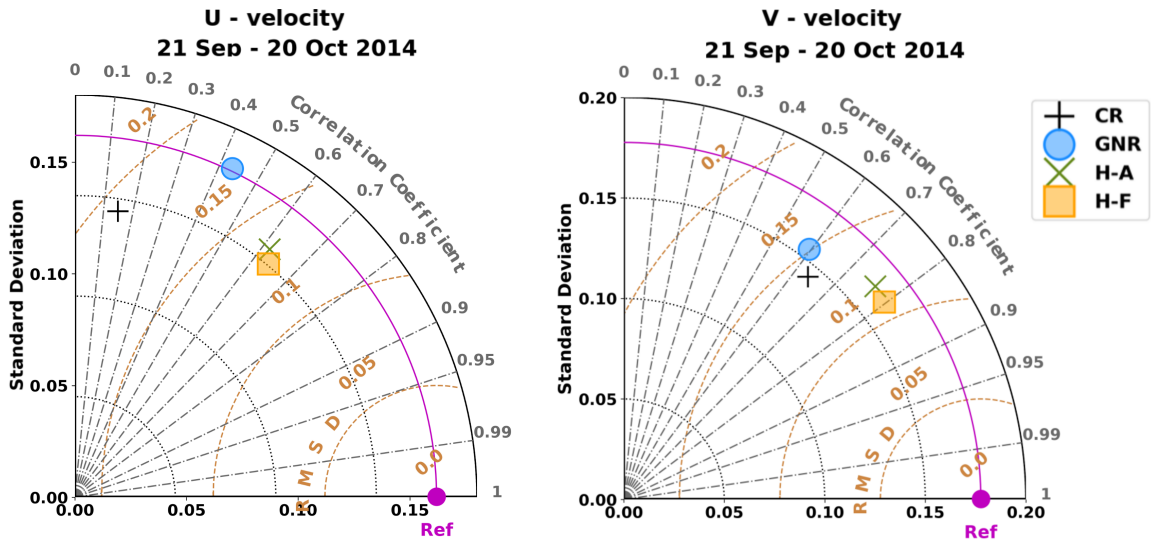


Figure 9: Same as Fig. 7 for velocities in the IC for the simulations spanning 21 September and 20 October 2014.

During the second period (1-30 August), the meridional currents were less intense than for the other simulation period, both in NR and CR. Furthermore, in NR, the currents in the western part of the IC were northward, contrary to CR and the area's mean dynamics. This is an anomalous situation circulation in the area, but that is known to happen few times every year. We aim to explore the potential impact of the HFR system extension in such situations, where the model could differ more from the observations. GNR degrades the forecasting of surface currents compared to CR. HFR observations are also needed to reduce the error and increase the correlation between the model simulations and the NR. When using HFR observations for the zonal velocity the correlation increases from 0.50 for the CR to 0.76 and 0.80, and the error is reduced by 23 and 29%, for H-A and H-F respectively.

The difference between using observation only from the actual coverage area and from the future one is significant for the meridional velocity. While H-A increases the correlation from 0.39 to 0.57 and reduces the RMSD by 17%, H-F further reduces the error by 19% with respect to H-A, meaning a total 32% total error reduction, with a correlation of 0.71.

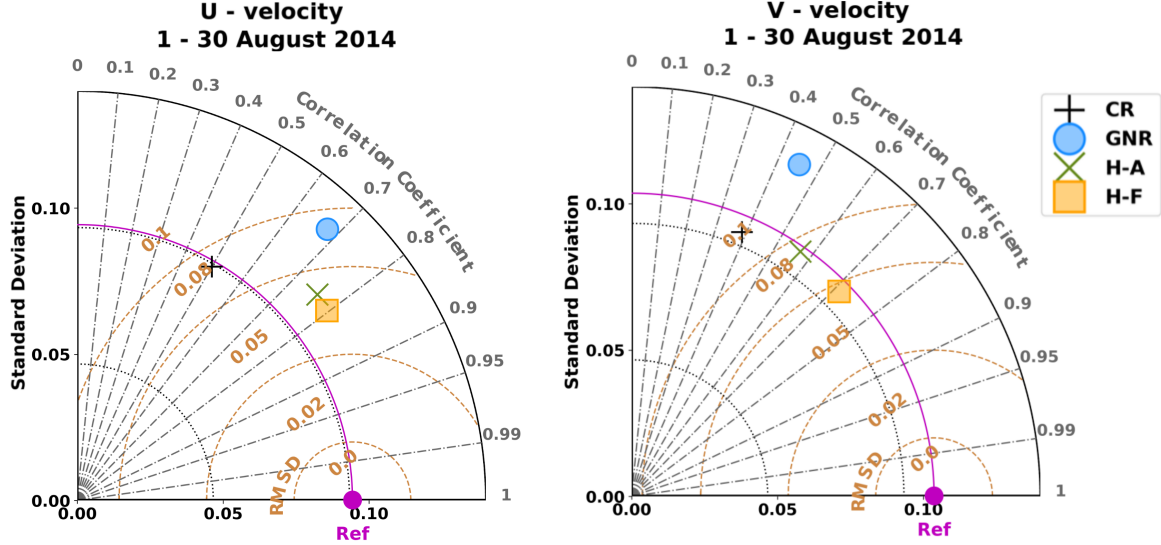


Figure 10: Same as Fig. 7 for velocities in the IC for the simulations spanning 1 and 30 August 2014.

3.3 Lagrangian validation

We focus our study on the region surrounding the IC, checking if the model can reproduce the LCS present in the NR when using DA. A qualitative analysis reveals that DA changes the LCS of the model with respect to the CR and can generate some of the structures present in the NR.

The LCS show areas of particle accumulation and barriers to transport. To better understand how DA impacts the dynamics in the area and how the transport patterns can be modified in the IC, we launch every 3 hours a set of 1000 particles in 4 different regions: i.e., north, south, east, and west of the IC. The regions are selected based on a geographical situation to evaluate the zonal and meridional flow exchanges.

Figure 11 shows the FSLE field for October 14 and the position of all the particles launched at the four sites every three hours since eight days before. The main LCS significantly differ between NR and CR in all the domain. CR shows an eddy in the southwest, centered at 1E 37.6N, that traps particles (in red) deployed at the south, while in NR, we can observe a loop-shape structure southwards. Red particles in NR move northeastwards between two LCS that make all particles flow uniformly until they arrive east of Ibiza island, where the field is less steady and with more diffusion, driving some of the particles southwards. This behavior is reproduced in the simulations using DA. H-F is the one that better reconstructs the LCS obtained with NR velocity fields.

The LCS present in the middle of the Ibiza Channel in NR are also well reproduced in both simulations where HFR data are assimilated. The orange particles flow eastwards until reaching this LCS, which acts as a barrier, splitting the possible track of the particles in two branches surrounding the island of Ibiza. This situation is not reproduced in CR, where all particles flow eastwards towards Ibiza crossing to the north side after a few days.

For the blue particles deployed in the eastern side of the IC we can observe how in NR most particles spread around Ibiza. For CR, the particles are quickly advected north-eastwards reaching the north of Mallorca island after a few days, following the LCS that joins the east parts of both islands. This structure is not so intense but still present in the data-assimilative simulations. However, most of the particles still remain close to Ibiza.

Finally, the set of particles deployed at the north (brown) are more dispersed in the DA simulations, along the LCS that is formed north of Ibiza at 39.2 N approximately. This structure is present in NR, but the particles slightly move during the eight days of simulation.

Figure 12 depicts the FSLE fields for 24 August, 2014 and the position of the particles, which were continuously launched every three hours since up to 8 days before. NR presents two big round shaped LCS in the south and east part of the plotted area, probably due to two respective eddies. CR also presents two big structures, but more displaced to the east. The zonal transport in the Mallorca-Ibiza channel will be restricted in the CR by a LCS that extends along the north coast of Mallorca and crossing the channel southward. On the other hand, the motion of particles is constrained

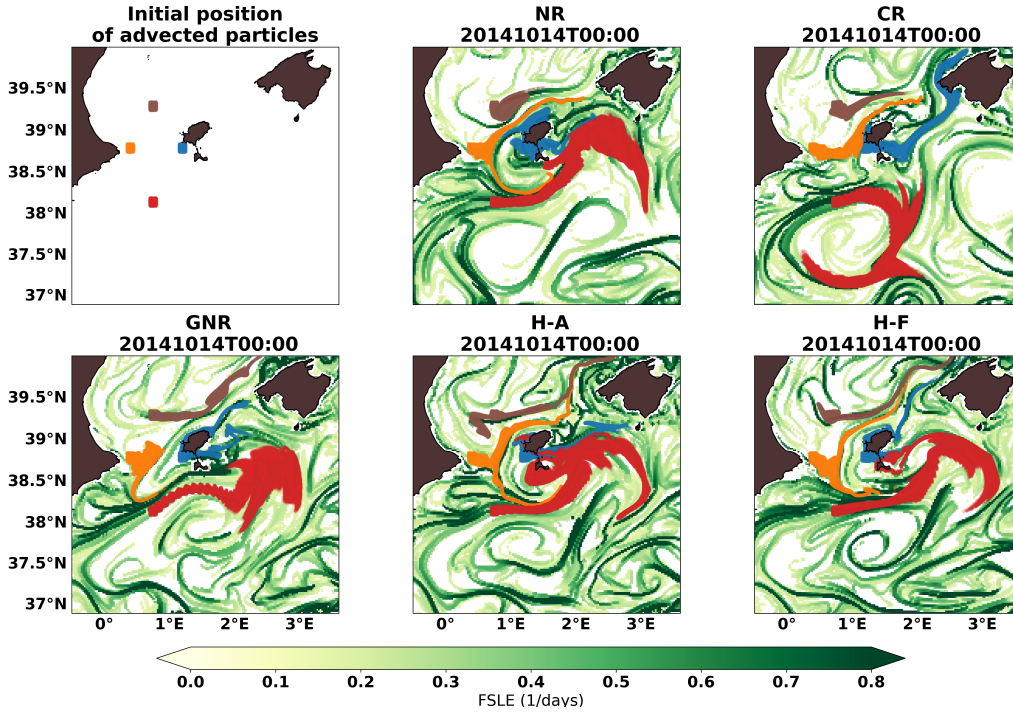


Figure 11: Lagrangian coherent structures from FSLE calculated backwards corresponding to 16-October-2014. Particles launched every 3 hours, starting in 6 October, from 4 different areas surrounding the IC are also shown with different colors.

meridionally in the IC, especially in the simulations with DA. In NR, the northern part of the eddy previously described would block this transport, while several structures limit it in all the DA simulations.

The most relevant difference found, regarding the transport of particles between the different simulations, are seen in the northern and eastern sides of the channel. For NR, orange particles flow northwards, as expected by the mean current observed during this period (Fig. 4), until they get blocked by a LCS, limiting the transport of brown particles at the south, that extend along the LCS in both directions. This behavior, that is not well reproduced in CR, can be reasonably well captured in H-F, where particles motions depict a very similar pattern, and also for H-A, but to a less extent. In this simulation, there is a slight displacement of some orange particles southwards at the initial stages, and we do not identify the left branch of the orange particles flowing northwards, as in NR and H-F.

4 Discussion

The experiments presented here apply an approach which has not been used before for the design and extension of a HFR system. The NR is validated to give realistic simulations and the innovation distribution of the pseudo-observations present a similar distribution to the real data. The results obtained in the OSSE framework in terms of error reduction and correlation increment are of the same order as of the ones obtained in the previous OSE work. For surface currents, there is a significant difference between the innovations obtained in OSE and OSSE, however we have seen that this difference is not systematic and depends on the analyzed period (Figure 6). Furthermore, when assimilating HFR, the error reduction and the increment in the correlation are also of the order of the one achieved in the OSE.

We have evaluated the impact on the surface currents in a wider area than that covered by the antennas, taking advantage of the full ocean state knowledge provided by the OSSE framework. It draws attention that the assimilation of only generic observing sources cannot correct the circulation in the area in the OSSE. In the previous OSE the assimilation of generic sources led to a good improvement compared to the CR. Even though the model's response to SLA, SST and Argo observations is very similar to that obtained with real observations, the circulation seems to have a highly ageostrophic component. Therefore, the correction of SSH and density fields is not able to correct the surface

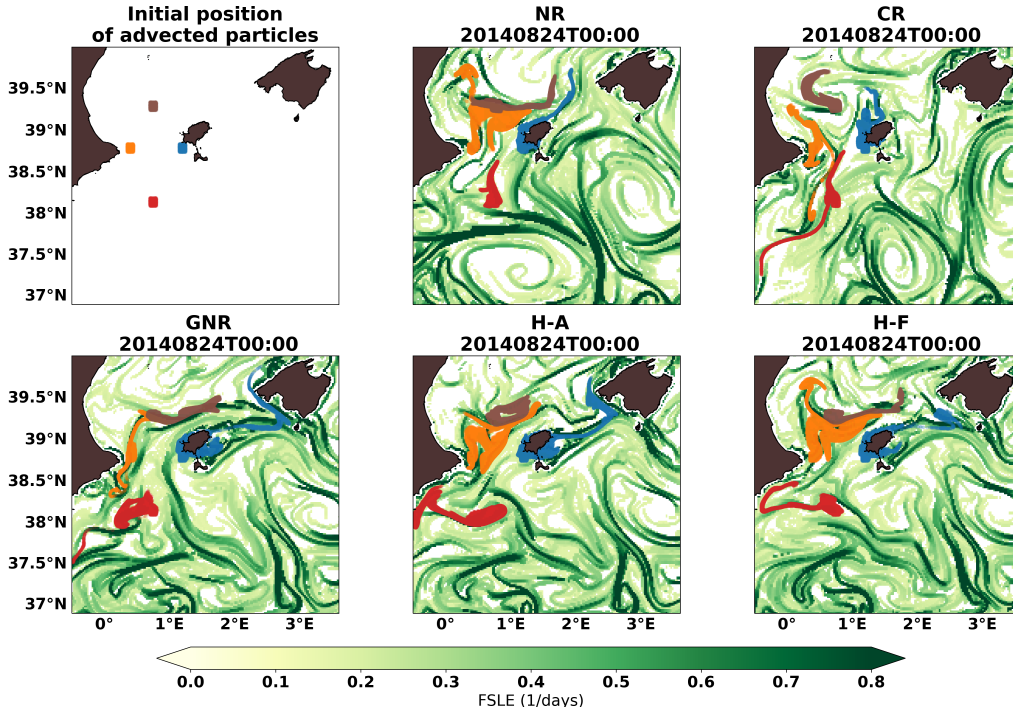


Figure 12: Lagrangian coherent structures from FSLE calculated backwards corresponding to 24-August-2014. Particles launched every 3 hours, starting in 16 August, from 4 different areas surrounding the IC are also shown with different colors.

currents in this region. This enhances the need of high-resolution surface current observations in coastal areas where satellite-derived geostrophic currents tend to fail [44].

The extension of the HFR system seems to be useful under certain conditions. The new antennas provide a moderate effect when NR and CR simulations reproduce similar circulation patterns. However, when both simulations present more differences, especially in the western side of the channel, having surface current observations of the full channel is key to improve the model dynamics. This can be interpreted as real situations in which the model is unable to reproduce the dynamics observed by the HFR system.

The observation error for the HFR has been considered the same in all the domain. It could be supposed that in areas covered by three antennas more radial observations will be used to generate a total observation, reducing the expected error. This approach, using a spatial variable error depending on the number of antennas that cover an area has been explored by some authors [43]. The improvement of the observations error, including correlated errors remains as a potential aspect to explore in future studies. Besides, the generation of all pseudo-observations could be made more realistic by generating the random noise based on a spatial structure, using a given correlation length.

We used a Lagrangian approach to evaluate the impact of data assimilation on the surface transport. The Lagrangian techniques, such as FSLE, have been increasingly being used in the last years. However, the effects of using a model field sequentially corrected through DA remains still poorly studied. As particles are advected, the DA simulation's discontinuities might impact the trajectories of the particles and the following computation of FSLE. Here we showed that simulations using DA behave in a similar way to those without DA. The particles tend to accumulate along LCS, which act as barriers to transport. The possible discontinuities do not seem to affect or create artifacts in the FSLE field or LCS. When comparing the FSLE fields computed for consecutive days, the transition between them is smooth. There is no significant difference when comparing the variation of LCS for two consecutive days with or without DA between them. Furthermore, the experiments performed here show how we can reconstruct some LCS present in the ocean state when assimilating observations. In particular, the use of HFR data for assimilation helps to recreate the LCS present in the NR and to correct the dynamics and the transport in the region, as was demonstrated with the advection of particles.

The four different areas in the IC from which we continuously deployed particles were selected in terms of their geographical location in the IC to evaluate the zonal and meridional transports in the channel and the connectivity

between the different regions. The study could also be complemented by analysing the trajectories of particles launched at different sites as the ones shown in this work. Besides, a further quantitative analysis would be desirable, although, establishing a metric for this kind of analysis is difficult and not extended in the literature. FSLE fields should not be compared point-wise, as little differences in the position of LCS could affect the results, leading to an erroneous interpretation. Developing a valid metric to quantify LCS differences remains as a future work.

OSSEs are an important tool to explore the capabilities of a future observing system design. Strictly, in scientific terms, it is always good to have as many observations as possible. However, as resources are limited, synergies between observing and modeling communities are needed to benefit mutually, and observing systems should rigorously be designed to meet user requirements and respond to societal needs [5]. For an optimal design of the observing system expansion further considerations could be taken into account. For instance, different locations for the antennas may be examined. For a final design, the decision should be jointly based on the scientific, and on the logistic and economic assessment, that are out of the scope of this work.

5 Conclusions

The objective of this study was to evaluate the impact of setting up a couple of antennas to complement the currently operating ones in the IC. We analyzed the impact of this new observing system on the transport properties through the LCS computation. The effect of data assimilation on the reconstruction of the LCS and its impact on the spreading of the advected particles has been assessed in a Lagrangian framework. A series of OSSEs assimilating HFR data along with traditional observing sources (SLA, SST, Argo) is presented here. The study is a continuation of the work from [16], where an OSE that is here used as reference to validate the OSSE framework was performed. The assessment of the OSSE is consistent with that of the reference OSE and the framework is considered suitable for the design and evaluation a future observing system.

The impact of a potential extension of the actual HFR system in the IC has been assessed. The two new antennas would provide a full coverage of the surface currents in the IC and could help to improve the forecasting of the circulation in the region. In circumstances where the flow regime represented by the model disagrees with the observed one, a diminution of up to 19% of the error can be expected when assimilating the future system observations, compared to the actual ones.

A Lagrangian analysis based on FSLE revealed that the use of model outputs corrected with DA are useful for this kind of analysis and are not significantly affected by possible field discontinuities. Furthermore, the analysis showed how the assimilation of HFR observations can help to reconstruct the LCS present in the NR and constrain the circulation in the IC.

Data availability

Data and numerical codes will be provided by the corresponding author upon request.

Authors contribution

JHL and BM conceptualized the OSSE. JHL, AO and IHC conceptualized the Lagrangian assessment. AS developed some of the Lagrangian tools used in this work. JHL conducted the experiments, performed the analysis and wrote the manuscript with the help of AO. All authors contributed in the discussion and review of the manuscript.

Competing interests

The authors declare that they have no conflict of interest.

Acknowledgements

This work was mostly done while Jaime Hernández-Laheras and Baptiste Mourre were at the SOCIB modelling facility. This research has been supported by the the EU Horizon 2020 JERICO-NEXT (grant agreement no. 654410) and EuroSea (grant agreement no. 862626). Alejandro Orfila acknowledges financial support from Projects LAMARCA (PID2021-123352OB-C31) funded by MICIN/AEI/10.13039/501100011033/ FEDER, UE; Tech2Coast (TED2021-130949B-I00) funded by MCIN/AEI/10.13039/ 501100011033 and by EU “NextGenerationEU/ PRTR” and LIFE

AdaptCalaMillor – LIFE21 GIC/ES/101074227. The authors are indebted to the Balearic Islands Coastal Observing System (SOCIB) for the HF-Radar data. The present research was carried out in the framework of the AEI accreditation “Maria de Maeztu Centre of Excellence” given to IMEDEA (CSIC-UIB) (CEX2021-001198).

References

- [1] Aguiar, E., Mourre, B., Juza, M., Reyes, E., Hernández-Lasheras, J., Cutolo, E., Mason, E., Tintoré, J., 2019. Multi-platform model assessment in the Western Mediterranean Sea : impact of downscaling on the surface circulation and mesoscale activity. *Ocean Dynamics*. doi:10.1007/s10236-019-01317-8Multi-platform.
- [2] Atlas, R., 1997. Atmospheric observations and experiments to assess their usefulness in data assimilation (gtspecial issue) data assimilation in meteorology and oceanography: theory and practice). *Journal of the Meteorological Society of Japan*. Ser. II 75, 111–130.
- [3] Ballabrera-Poy, J., Hackert, E., Murtugudde, R., Busalacchi, A.J., 2007. An observing system simulation experiment for an optimal moored instrument array in the tropical indian ocean. *Journal of Climate* 20, 3284–3299.
- [4] Benkiran, M., Ruggiero, G., Greiner, E., Le Traon, P.Y., Rémy, E., Lellouche, J.M., Bourdallé-Badie, R., Drillet, Y., Tchonang, B., 2021. Assessing the Impact of the Assimilation of SWOT Observations in a Global High-Resolution Analysis and Forecasting System Part 1: Methods. *Frontiers in Marine Science* 8, 1–19. doi:10.3389/fmars.2021.691955.
- [5] Davidson, F., Alvera-Azcárate, A., Barth, A., Brassington, G.B., Chassignet, E.P., Clementi, E., De Mey-Frémaux, P., Divakaran, P., Harris, C., Hernandez, F., Hogan, P., Hole, L.R., Holt, J., Liu, G., Lu, Y., Lorente, P., Maksymczuk, J., Martin, M., Mehra, A., Melsom, A., Mo, H., Moore, A., Oddo, P., Pascual, A., Pequignet, A.C., Kourafalou, V., Ryan, A., Siddorn, J., Smith, G., Spindler, D., Spindler, T., Stanev, E.V., Staneva, J., Storto, A., Tanajura, C., Vinayachandran, P.N., Wan, L., Wang, H., Zhang, Y., Zhu, X., Zu, Z., 2019. Synergies in operational oceanography: The intrinsic need for sustained ocean observations. *Frontiers in Marine Science* 6, 1–18. doi:10.3389/fmars.2019.00450.
- [6] deYoung, B., Visbeck, M., Filho, M.C., Baringer, M.O., Black, C.A., Buch, E., Canonico, G., Coelho, P., Duha, J.T., Edwards, M., Fischer, A.S., Fritz, J.S., Ketelhake, S., Muelbert, J.H., Monteiro, P., Nolan, G., O’Rourke, E., Ott, M., Le Traon, P.Y., Pouliquen, S., Pinto, I.S., Tanhua, T., Velho, F., Willis, Z., 2019. An integrated all-Atlantic ocean observing system in 2030. *Frontiers in Marine Science* 6, 1–22. doi:10.3389/fmars.2019.00428.
- [7] Díaz-Barroso, L., Hernández-Carrasco, I., Orfila, A., Reglero, P., Balbín, R., Hidalgo, M., Tintoré, J., Alemany, F., Álvarez-Berastegui, D., 2022. Singularities of surface mixing activity in the western mediterranean influence bluefin tuna larval habitats. *Marine Ecology Progress Series* 685, 69–84.
- [8] d’Ovidio, F., Fernández, V., Hernández-García, E., López, C., 2004. Mixing structures in the Mediterranean Sea from finite-size Lyapunov exponents. *Geophysical Research Letters* 31, 1–4. doi:10.1029/2004GL020328.
- [9] Farcy, P., Durand, D., Charria, G., Painting, S.J., Tamminem, T., Collingridge, K., Grémare, A.J., Delauney, L., Puillat, I., 2019. Toward a European coastal observing network to provide better answers to science and to societal challenges; the JERICO research infrastructure. *Frontiers in Marine Science* 6, 1–13. doi:10.3389/fmars.2019.00529.
- [10] Gasparin, F., Guinehut, S., Mao, C., Mirouze, I., Rémy, E., King, R.R., Hamon, M., Reid, R., Storto, A., Le Traon, P.Y., Martin, M.J., Masina, S., 2019. Requirements for an Integrated in situ Atlantic Ocean Observing System From Coordinated Observing System Simulation Experiments. *Frontiers in Marine Science* 6. doi:10.3389/fmars.2019.00083.
- [11] Guinehut, S., Le Traon, P.Y., Larnicol, G., Philipps, S., 2004. Combining Argo and remote-sensing data to estimate the ocean three-dimensional temperature fields - A first approach based on simulated observations. *Journal of Marine Systems* 46, 85–98. doi:10.1016/j.jmarsys.2003.11.022.
- [12] Halliwell, J.R., Srinivasan, A., Kourafalou, V., Yang, H., Willey, D., Le Hénaff, M., Atlas, R., 2014. Rigorous evaluation of a fraternal twin ocean OSSE system for the open Gulf of Mexico. *Journal of Atmospheric and Oceanic Technology* 31, 105–130. doi:10.1175/JTECH-D-13-00011.1.
- [13] Hernández-Carrasco, I., López, C., Hernández-García, E., Turiel, A., 2011. How reliable are finite-size Lyapunov exponents for the assessment of ocean dynamics? *Ocean Modelling* 36, 208–218. doi:10.1016/j.ocemod.2010.12.006.
- [14] Hernandez-Carrasco, I., López, C., Hernandez-García, E., Turiel, A., 2012. Seasonal and regional characterization of horizontal stirring in the global ocean. *Journal of Geophysical Research: Oceans* 117, 1–12. doi:10.1029/2012JC008222.

- [15] Hernández-Carrasco, I., Orfila, A., Rossi, V., Garçon, V., 2018. Effect of small scale transport processes on phytoplankton distribution in coastal seas. *Scientific Reports* 8, 1–13. doi:10.1038/s41598-018-26857-9.
- [16] Hernandez-Lasheras, J., Mourre, B., Orfila, A., Santana, A., Reyes, E., Tintoré, J., 2021. Evaluating High-Frequency radar data assimilation impact in coastal ocean operational modelling. *Ocean Science Discussions* , 1–29doi:10.5194/os-2021-34.
- [17] Hernández-Carrasco, I., Orfila, A., 2018. The role of an intense front on the connectivity of the western mediterranean sea: The cartagena-tenes front. *Journal of Geophysical Research: Oceans* 123, 4398–4422. doi:10.1029/2017JC013613.
- [18] Heslop, E.E., Ruiz, S., Allen, J., López-jurado, J.L., Renault, L., Tintoré, J., 2012. Autonomous underwater gliders monitoring variability at “choke points” in our ocean system: A case study in the Western Mediterranean Sea. *Geophysical Research Letters* 39, 1–6. doi:10.1029/2012GL053717.
- [19] Hoffman, R.N., Atlas, R., 2016. Future observing system simulation experiments. *Bulletin of the American Meteorological Society* 97, 1601–1616.
- [20] Juza, M., Mourre, B., Renault, L., Gómara, S., Sebastian, K., López, S.L., Borrueco, B.F., Beltran, J.P., Troupin, C., Tomás, M.T., Heslop, E., Casas, B., Tintoré, J., 2016. Operational SOCIB forecasting system and multi-platform validation in the Western Mediterranean. *Journal of Operational Oceanography* , 9231doi:10.1002/2013JC009231.
- [21] Kai, E.T., Rossi, V., Sudre, J., Weimerskirch, H., Lopez, C., Hernandez-Garcia, E., Marsac, F., Garçon, V., 2009. Top marine predators track lagrangian coherent structures. *Proceedings of the National Academy of Sciences* 106, 8245–8250.
- [22] Kourafalou, V., De Mey, P., Le Hénaff, M., Charria, G., Edwards, C., He, R., Herzfeld, M., Pascual, a., Stanev, E., Tintoré, J., Usui, N., van der Westhuysen, a., Wilkin, J., Zhu, X., 2015. Coastal Ocean Forecasting: system integration and evaluation. *Journal of Operational Oceanography* 8, s127–s146. doi:10.1080/1755876X.2015.1022336.
- [23] Lange, M., Van Sebille, E., 2017. Parcels v0.9: Prototyping a Lagrangian Ocean Analysis framework for the petascale age. *arXiv* , 4175–4186doi:10.5194/gmd-2017-167.
- [24] Le Traon, P.Y., 2013. From satellite altimetry to Argo and operational oceanography: Three revolutions in oceanography. *Ocean Science* 9, 901–915. doi:10.5194/os-9-901-2013.
- [25] Le Traon, P.Y., Reppucci, A., Alvarez Fanjul, E., Aouf, L., Behrens, A., Belmonte, M., Bentamy, A., Bertino, L., Brando, V.E., Kreiner, M.B., Benkiran, M., Carval, T., Ciliberti, S.A., Claustre, H., Clementi, E., Coppini, G., Cossarini, G., De Alfonso Alonso-Muñoyerro, M., Delamarche, A., Dibarboure, G., Dinessen, F., Drevillon, M., Drillet, Y., Faugere, Y., Fernández, V., Fleming, A., Garcia-Hermosa, M.I., Sotillo, M.G., Garric, G., Gasparin, F., Giordan, C., Gehlen, M., Gregoire, M.L., Guinehut, S., Hamon, M., Harris, C., Hernandez, F., Hinkler, J.B., Hoyer, J., Karvonen, J., Kay, S., King, R., Lavergne, T., Lemieux-Dudon, B., Lima, L., Mao, C., Martin, M.J., Masina, S., Melet, A., Buongiorno Nardelli, B., Nolan, G., Pascual, A., Pistoia, J., Palazov, A., Piolle, J.F., Pujol, M.I., Pequignet, A.C., Peneva, E., Pérez Gómez, B., Petit de la Villeon, L., Pinardi, N., Pisano, A., Pouliquen, S., Reid, R., Remy, E., Santoleri, R., Siddorn, J., She, J., Staneva, J., Stoffelen, A., Tonani, M., Vandenbulcke, L., von Schuckmann, K., Volpe, G., Wettre, C., Zacharioudaki, A., 2019. From Observation to Information and Users: The Copernicus Marine Service Perspective. *Frontiers in Marine Science* 6. doi:10.3389/fmars.2019.00234.
- [26] Lehahn, Y., d’Ovidio, F., Lévy, M., Heifetz, E., 2007. Stirring of the northeast Atlantic spring bloom: A Lagrangian analysis based on multisatellite data. *Journal of Geophysical Research: Oceans* 112, 1–15. doi:10.1029/2006JC003927.
- [27] Lekien, F., Coulliette, C., Mariano, A.J., Ryan, E.H., Shay, L.K., Haller, G., Marsden, J., 2005. Pollution release tied to invariant manifolds: A case study for the coast of florida. *Physica D: Nonlinear Phenomena* 210, 1–20.
- [28] Moltmann, T., Turton, J., Zhang, H.M., Nolan, G., Gouldman, C., Griesbauer, L., Willis, Z., Piniella, A.M., Barrell, S., Andersson, E., Gallage, C., Charpentier, E., Belbeoch, M., Poli, P., Rea, A., Burger, E.F., Legler, D.M., Lumpkin, R., Meinig, C., O’Brien, K., Saha, K., Sutton, A., Zhang, D., Zhang, Y., 2019. A Global Ocean Observing System (GOOS), delivered through enhanced collaboration across regions, communities, and new technologies. *Frontiers in Marine Science* 6, 1–21. doi:10.3389/fmars.2019.00291.
- [29] Mourre, B., Aguiar, E., Juza, M., Hernandez-Lasheras, J., Reyes, E., Heslop, E., Escudier, R., Cutolo, E., Ruiz, S., Mason, E., Pascual, A., Tintoré, J., 2018. Assessment of High-Resolution Regional Ocean Prediction Systems Using Multi-Platform Observations: Illustrations in the Western Mediterranean Sea. *New Frontiers in Operational Oceanography* , 663–694doi:10.17125/gov2018.ch24.

- [30] Pascual, A., Bouffard, J., Ruiz, S., Buongiorno Nardelli, B., Vidal-Vijande, E., Escudier, R., Sayol, J.M., Orfila, A., 2013. Recent improvements in mesoscale characterization of the western Mediterranean Sea: synergy between satellite altimetry and other observational approaches. *Scientia Marina* 77, 19–36. doi:10.3989/scimar.03740.15A.
- [31] Pinot, J.M., Tintoré, J., Gomis, D., 1994. Quasi-synoptic mesoscale variability in the Balearic Sea. *Deep-Sea Research Part I* 41, 897–914. doi:10.1016/0967-0637(94)90082-5.
- [32] Pinot, J.M., Tintoré, J., Gomis, D., 1995. Multivariate analysis of the surface circulation in the Balearic Sea. *Progress in Oceanography* 36, 343–376. doi:10.1016/0079-6611(96)00003-1.
- [33] Ryabinin, V., Barbière, J., Haugan, P., Kullenberg, G., Smith, N., McLean, C., Troisi, A., Fischer, A.S., Aricò, S., Aarup, T., Pissierssens, P., Visbeck, M., Enevoldsen, H., Rigaud, J., 2019. The UN decade of ocean science for sustainable development. *Frontiers in Marine Science* 6. doi:10.3389/fmars.2019.00470.
- [34] Sakov, P., Oke, P.R., 2008. Objective array design: Application to the tropical indian ocean. *Journal of atmospheric and oceanic technology* 25, 794–807.
- [35] Shadden, S.C., Lekien, F., Marsden, J.E., 2005. Definition and properties of lagrangian coherent structures from finite-time lyapunov exponents in two-dimensional aperiodic flows. *Physica D: Nonlinear Phenomena* 212, 271–304.
- [36] Shchepetkin, A.F., McWilliams, J.C., 2005. The regional oceanic modeling system (ROMS): A split-explicit, free-surface, topography-following-coordinate oceanic model. *Ocean Modelling* 9, 347–404. doi:10.1016/j.ocemod.2004.08.002.
- [37] Simoncelli, S., Fratianni, C., Pinardi, N., Grandi, A., Drudi, M., Oddo, P., Dobricic, S., 2017. Mediterranean Sea physical reanalysis (MEDREA 1987-2015) (Version 1)[Data set]. Copernicus Monitoring Environment Marine Service (CMEMS) doi:10.25423/medsea{_}reanalysis{_}phys{_}006{_}004.
- [38] Sloyan, B.M., Wilkin, J., Hill, K.L., Chidichimo, M.P., Cronin, M.F., Johannessen, J.A., Karstensen, J., Krug, M., Lee, T., Oka, E., Palmer, M.D., Rabe, B., Speich, S., Von Schuckmann, K., Weller, R.A., Yu, W., 2019. Evolving the global ocean observing system for research and application services through international coordinatio. *Frontiers in Marine Science* 6. doi:10.3389/fmars.2019.00449.
- [39] Smith, W.H., Sandwell, D.T., 1997. Global Sea Floor Topography from SATellite Altimetry and Ship Depth Soundings. *Science* 2, 209 –215.
- [40] Tintoré, J., Lana, A., Marmain, J., Fernández, V., Casas, B., Reyes, E., 2012. HF Radar Ibiza data from date 2012-06-01. doi:https://doi.org/10.25704/17GS-2B59.
- [41] Tintoré, J., Pinardi, N., Álvarez-Fanjul, E., Aguiar, E., Álvarez-Berastegui, D., Bajo, M., Balbin, R., Bozzano, R., Nardelli, B.B., Cardin, V., Casas, B., Charcos-Llorens, M., Chiggiato, J., Clementi, E., Coppini, G., Coppola, L., Cossarini, G., Deidun, A., Deudero, S., D’Ortenzio, F., Drago, A., Drudi, M., El Serafy, G., Escudier, R., Farcy, P., Federico, I., Fernández, J.G., Ferrarin, C., Fossi, C., Frangoulis, C., Galgani, F., Gana, S., García Lafuente, J., Sotillo, M.G., Garreau, P., Gertman, I., Gómez-Pujol, L., Grandi, A., Hayes, D., Hernández-Lasheras, J., Herut, B., Heslop, E., Hilmi, K., Juza, M., Kallos, G., Korres, G., Lecci, R., Lazzari, P., Lorente, P., Liubartseva, S., Louanchi, F., Malacic, V., Mannarini, G., March, D., Marullo, S., Mauri, E., Meszaros, L., Mourre, B., Mortier, L., Muñoz-Mas, C., Novellino, A., Obaton, D., Orfila, A., Pascual, A., Pensieri, S., Pérez Gómez, B., Pérez Rubio, S., Perivoliotis, L., Petihakis, G., de la Villéon, L.P., Pistoia, J., Poulain, P.M., Pouliquen, S., Prieto, L., Raimbault, P., Reglero, P., Reyes, E., Rotllan, P., Ruiz, S., Ruiz, J., Ruiz, I., Ruiz-Orejón, L.F., Salihoglu, B., Salon, S., Sammartino, S., Sánchez Arcilla, A., Sannino, G., Sannino, G., Santoleri, R., Sardá, R., Schroeder, K., Simoncelli, S., Sofianos, S., Sylaios, G., Tanhua, T., Teruzzi, A., Testor, P., Tezcan, D., Torner, M., Trotta, F., Umgiesser, G., von Schuckmann, K., Verri, G., Vilibic, I., Yucel, M., Zavatarelli, M., Zodiatis, G., 2019. Challenges for Sustained Observing and Forecasting Systems in the Mediterranean Sea. *Frontiers in Marine Science* 6. doi:10.3389/fmars.2019.00568.
- [42] Undén, P., Rontu, L., Järvinen, H., Lynch, P., Calvo, J., Cats, G., Cuxart, J., Eerola, K., Fortelius, C., Garcia-Moya, J.A., Jones, C., Lenderlink, G., McDonald, A., McGrath, R., Navasques, B., Nielsen, N.W., Ødegaard, V., Rodriguez, E., Rummukainen, M., Rööm, R., Sattler, K., Sass, B.H., Savijärvi, H., Schreur, B.W., Sigg, R., The, H., Tijn, A., 2002. High Resolution Limited Area Model, HIRLAM-5 Scientific Documentation. Technical Report December. SMHI. Norrköping, SWEDEN.
- [43] Vandenbulcke, L., Beckers, J.m., Barth, A., 2017. Correction of inertial oscillations by assimilation of HF radar data in a model of the Ligurian Sea. *Ocean Dynamics* , 117–135doi:10.1007/s10236-016-1012-5.
- [44] Vignudelli, S., Birol, F., Benveniste, J., Fu, L.L., Picot, N., Raynal, M., Roinard, H., 2019. Satellite Altimetry Measurements of Sea Level in the Coastal Zone. volume 40. Springer Netherlands. doi:10.1007/s10712-019-09569-1.

- [45] Visbeck, M., 2018. Ocean science research is key for a sustainable future. *Nature Communications* 9, 1–4. doi:10.1038/s41467-018-03158-3.